Available online at www.sciencedirect.com
SCIENCE DIRECT
Bioorganic & Medicinal Chemistry 14 (2006) 3563–3570
Bioorganic & Medicinal Chemistry

# Design, synthesis, and evaluation of new type of L-amino acids containing pyridine moiety as nitric oxide synthase inhibitor

Ryosuke Ijuin, Naoki Umezawa and Tsunehiko Higuchi*

*Graduate School of Pharmaceutical Sciences, Nagoya City University, 3-1 Tanabe-dori, Mizuho-ku, Nagoya 467-8603, Japan*

Received 14 November 2005; revised 6 January 2006; accepted 7 January 2006
Available online 8 February 2006

**Abstract**—New amino acids **7**–**12** were designed and synthesized as candidate inhibitors of human nitric oxide synthase (NOS). The 2-aminopyridine-containing L-amino acids **8** had potent inhibitory activity toward all of the human NOS isozymes. However, the regioisomers **9** and **10**, and 2-methylpyridine-containing compound **11** had much lower inhibitory activity. Human NOS isozymes were also inhibited by **7**, which lacks an amino group on the pyridine moiety. A computational docking study was carried out to investigate the mechanism of the inhibitory effect.


## 1. Introduction

Nitric oxide synthase (NOS) catalyzes the oxidation of a guanidino nitrogen of L-arginine to nitric oxide (NO) with concomitant formation of L-citrulline.[1] NO is an important signaling molecule involved in a wide range of physiological functions, as well as pathophysiological states.[2–4] Three major isozymes of NOS have been identified. The endothelial isozyme (eNOS),[5] which is constitutive and tightly regulated by $Ca^{2+}$ and calmodulin (CaM), plays a key role in maintaining normal blood pressure.[6] The inducible isozyme (iNOS)[7] is expressed in response to endotoxin and inflammatory cytokines in macrophages, in vascular endothelial and smooth muscle cells, and in many other cell types. Because iNOS is often expressed at high levels and is essentially unregulated once expressed, locally high, and therefore cytotoxic concentrations of NO can be generated. Neuronal NOS (nNOS)[8] as with eNOS, is constitutive and tightly regulated by $Ca^{2+}$/CaM. Although nNOS normally generates low levels of NO for intercellular signaling in the nervous system, overstimulation of nNOS is implicated in ischemia-reperfusion injury following stroke, migraine headache, pain, and several neurodegenerative disorders.

Structural analogs of L-arginine, the natural substrate of NOS, have been shown to inhibit the various forms of NOS, and non-amino acid inhibitors of NOS have also been reported.[9] For example, *S*-methyl-isothiocitrulline (L-MIT **1**),[10] *N*-iminoethyl-L-ornithine (L-NIO **2**),[11] and *N*-iminoethyl-L-lysine (L-NIL **3**)[12] are arginine analogs with potent inhibitory activities toward all three NOS isozymes, while 1400W (**4**)[13] is a non-amino acid type inhibitor that is iNOS-selective. We have previously designed two types of NOS inhibitors based on the working hypothesis that each NOS isozyme has a different hydrophobic region at its L-arginine recognition site. First, we designed a dipeptide-type NOS inhibitor (**5**),[14,15] which has a phenylalanine moiety at the C-terminal of L-MIT, and found that it is an iNOS-selective inhibitor. Next, we designed **6**,[16] which has an alkyl moiety at the 3-position of L-MIT, we found that the 3-(*R*)-methyl derivative **6** has no inhibitory effect on eNOS, but inhibits both nNOS and iNOS, whereas the 3-(*S*)-methyl derivative inhibits all the NOS isozymes (Fig. 1). These results suggested that arginine analogs with a hydrophobic substituent could be isozyme-selective inhibitors. To examine the contribution of hydrophobic substituents near the guanidino group of the substrate, we have newly designed pyridine ring-containing arginine analogs (**7**–**12**) and investigated their structure–activity relationship (Fig. 2). These types of aminopyridines should be more stable than those containing an *S*-alkylated isothiourea moiety. Recently, Connolly et al. reported 2-aminopyridines as iNOS-selective inhibitors.[17] Here, we describe the synthesis of new 2-aminopyridine-type arginine analogs and the

*Keywords*: Nitric oxide synthase; Inhibitor; Human; Pyridine; Picoline; Design; Synthesis; $IC_{50}$; Regioisomer; 2-Aminopyridine; Cysteine; Arginine; Amino acid; Citrulline assay; Computational docking study; Isozyme; Structure–activity relationship; Competitive; Nitric oxide.
* Corresponding author. Tel./fax: +81 52 836 3435; e-mail: higuchi@phar.nagoya-cu.ac.jp

0968-0896/$ - see front matter © 2006 Elsevier Ltd. All rights reserved.
doi:10.1016/j.bmc.2006.01.020

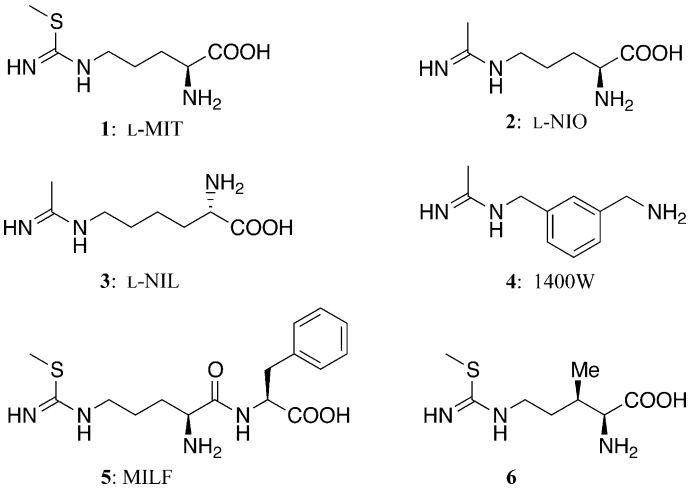


**Figure 1.** Structures of NOS inhibitors.

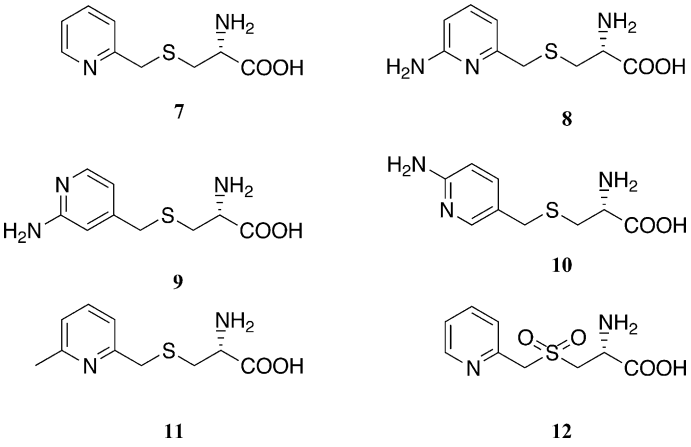


**Figure 2.** Designs of NOS inhibitors.

evaluation of their inhibitory activity toward the three recombinant human NOS isozymes. A docking study was conducted to throw light on the substituent.

## 2. Results and discussion

### 2.1. Chemistry

The first step in the synthesis was protection of 2-amino picolines **13a–c**. The protected picolines (**14a–c**) were easily converted to bromomethyl derivatives **15a–c**.[18] These compounds were too unstable to isolate, so we used them without further purification. 2-Picoline (**16d**) and 2,6-lutidine (**16e**) were converted to bromomethyl derivatives **17d,e** (Scheme 1). Protected cysteine **18** was obtained from L-cystine according to the literature.[19,20] Reaction of **15a–c** or **17d,e** with **18** gave pyridine ring-containing protected amino acids (**19a–e**). Deprotection of **19a–e** afforded the desired amino acids (**7–11**) (Scheme 2). We also synthesized the sulfonyl compound **20**, by oxidation of **19d**, and **12** was obtained by deprotection of **20** (Scheme 3). The route allows ready variation of the heteroaromatic groups because a number of bromomethylated heteroarenes are readily available.

### 2.2. Biological evaluation

Human NOS isozymes were expressed in Sf-9 (a *Spodoptera frugiperda* insect cell line). Recombinant human NOS activity was measured by monitoring the conversion of [$^{14}$C]-L-Arg to [$^{14}$C]-L-Cit.[21] The $IC_{50}$ values of synthesized compounds were calculated from the concentration dependence of the inhibitory activity (Table 1). Compound **7**, without an amino group on the pyridine ring, inhibited all the human NOS isozymes ($IC_{50}$ values: nNOS 2 μM, iNOS 0.5 μM, and eNOS 4.8 μM), with slight selectivity for iNOS (entry 1). Compound **8** had potent inhibitory activity toward each NOS isozyme ($IC_{50}$ values: nNOS 0.06 μM, iNOS 0.1 μM, and eNOS 0.02 μM), and potency was comparable to that of L-MIT **1** (entries 2 and 7). The 2-aminopyridine group seems to provide higher affinity for NOS than does a simple pyridine group. Compound **9**, with the amino acid moiety at the 4-position, had much weaker inhibitory activity than **8** (entry 3). Moreover, compound **10**, substituted at the 5-position, showed

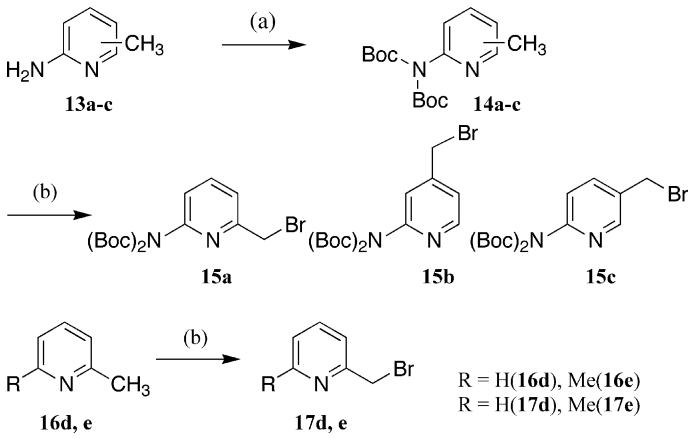


**Scheme 1.** Reagents: (a) $Boc_2O$, DMAP, *N*,*N*-diisopropylethylamine, $CH_2Cl_2$, **14a** 22%, **14b** 33%, **14c** 24%; (b) NBS, BPO, $CCl_4$, **17d** 28%, **17e** 31%.

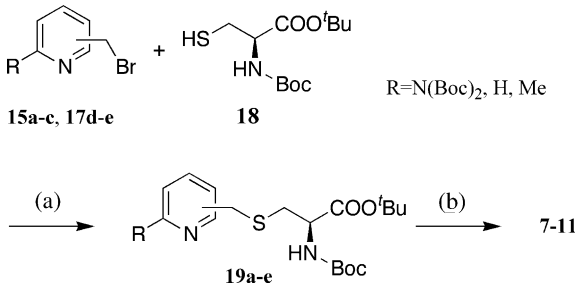


**Scheme 2.** Reagents and conditions: (a) **17**, *N*,*N*-diisopropylethylamine, $CH_2Cl_2$, rt, 16 h, **19a** 35% in two steps, **19b** 58% in two steps, **19c** 53% in two steps, **19d** 71%, (b) HCl–dioxane, rt, 12 h. All compounds were obtained in quantitative yield.

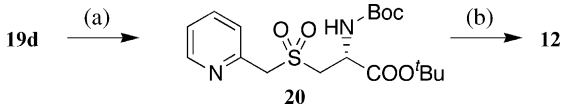


**Scheme 3.** Reagents and conditions: (a) *m*-CPBA, $CH_2Cl_2$, 32%; (b) HCl–dioxane, rt, 12 h, quant.

**Table 1.** $IC_{50}$ values (μM) for inhibition of human NOS isozymes[a]

| Entry | Compound | nNOS[b] | iNOS[b] | eNOS[b] |
|---|---|---|---|---|
| 1 | **7** | 2 | 0.5 | 4.8 |
| 2 | **8** | 0.06 | 0.1 | 0.02 |
| 3 | **9** | 90 | 50 | 42 |
| 4 | **10** | 390 | 120 | 400 |
| 5 | **11** | 500 | 140 | 260 |
| 6 | **12** | 100 | 45 | 200 |
| 7 | **1**[c] | 0.06 | 0.3 | 0.4 |
| 8 | **3**[d] | 61 | 5 | 138 |
| 9 | **5**[c] | 36 | 3.9 | >1000[f] |
| 10 | **±6**[e] | 38 | 110 | >1000[f] |

[a] Human NOS activity was measured by monitoring the conversion of [$^{14}$C]-L-Arg to [$^{14}$C]-L-Cit.
[b] Human NOS isozymes were expressed in Sf-9 cells.
[c] Data from Ref. 15.
[d] Data from Ref. 12.
[e] Data from Ref. 16.
[f] Not inhibited by 50% at concentrations up to 1 mM inhibitor.

**Table 2.** Kinetic constants (μM) of obtained amino acids for human NOS isozymes[a]

| Entry | Compound | nNOS[b] | iNOS[b] | eNOS[b] |
|---|---|---|---|---|
| 1 | L-Arg ($K_m$)[c] | 1.5 | 4.0 | 2.0 |
| 2 | **7** | 16 | 2 | 3.7 |
| 3 | **8** | 1.5 | 9.5 | 0.5 |

[a] $K_i$ values were analyzed by means of Dixon analysis. Measurement of human NOS activity under initial velocity conditions is described in Section 4.
[b] Human NOS isozymes were expressed in Sf-9 cells.
[c] Data from Ref. 15.

dramatically decreased inhibitory activity (entry 4). Compound **11**, with a methyl group instead of an amino group on the pyridine ring of **8**, had low inhibitory activity toward each NOS isozyme (entry 5). This result indicates that the amino group plays an important role in recognition at the NOS active site. Moreover, compound **12**, with a sulfonyl linker, also had a low inhibitory activity (entry 6). We also measured the kinetic constant to reveal the manner of inhibition. Dixon analysis[22] for the inhibition by **7** and **8** was carried out and the results indicated that they are competitive inhibitors of the three human NOS isozymes (Table 2 and

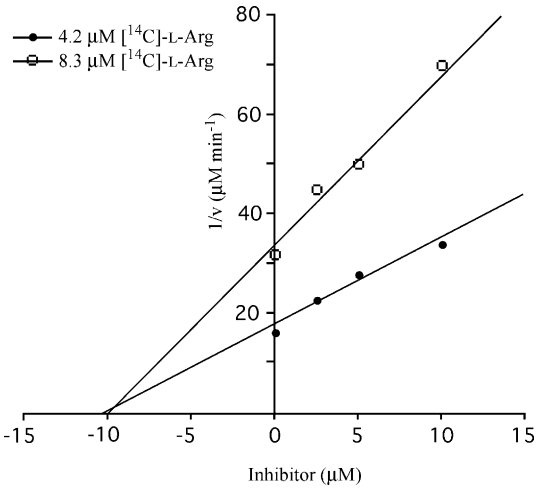


**Figure 3.** Dixon analysis of inhibition of human iNOS by **8**. Measurement of human iNOS activity under initial velocity conditions is [$^{14}$C]-L-arginine concentration was 4.2 or 8.3 μM.

Fig. 3). We found that the direction of the amidino moiety linked with the 2-aminopyridine in the amino acid greatly affects the inhibitory activity. This result strongly suggests that it is important to direct the amidino moiety appropriately for binding to the carboxyl group of Glu 377 that should fix the guanidino group of L-arginine. In order to investigate this hypothesis, we conducted docking calculations.

### 2.3. Docking study

To study the binding modes of **8** and **10** to the active site, we calculated the minimum energy conformations of **8** and **10** docked into a model based on the crystal structure of human iNOS (PDB code 1NSI)[23] using the software package MacroModel 8.1, and we compared the results with those obtained for L-NIL (**3**) (Fig. 4). The obtained structures were similar in their amino acid backbone orientation and showed good overlap with **3** in the iNOS active site (Fig. 4a). There is a high degree of similarity among the binding modes to iNOS of the amino acid backbone in **8** and **10**. However, in the case of **10**, the amino group on the pyridine ring cannot be overlapped with that of **3** or **8** (Fig. 4b). This result is consistent with the difference of NOS-inhibitory activity between **8** and **10**. Next, we calculated hydrogen-bonding interactions between iNOS residues and inhibitors **8** and **10** to investigate the effects of the amino group on the pyridine ring (Figs. 5a and b, 6). In the case of **8**, a hydrogen atom of $\alpha$-$NH_3^+$ was located at 1.55 Å from heme propionate, an oxygen atom of carboxylate was located at 2.11 Å from a hydrogen atom of Arg 388 and a hydrogen atom of pyridinium ion was located at 1.44 Å from an oxygen atom of Glu 377. On the other hand, in the case of **10**, hydrogen of $\alpha$-$NH_3^+$ was located at 1.61 Å from heme propionate, and oxygen of carboxylate was located at 2.24 Å from hydrogen of Arg 388. The pyridinium ion of **10** was located too far from Glu 377 for hydrogen-bonding to occur. It is suggested that **10** has weak affinity for the binding site because it has less hydrogen-bonding and ionic interaction with iNOS residues than does **8**. These results are consistent with the difference of inhibitory activity between **8** and **10**. We also calculated the minimum energy conformations of **21** (Fig. 7), which are known as iNOS selective inhibitor ($IC_{50}$ values for human NOS; nNOS 177 μM, iNOS 2.19 μM, and eNOS 544 μM),[24] docked into a model. We calculated hydrogen-bonding interactions between iNOS residues and the inhibitor **21** to compare with **8** and **10**. In the case of **21**, hydrogen atom of $\alpha$-$NH_3^+$ was located at 1.64 Å from heme propionate, an oxygen atom of

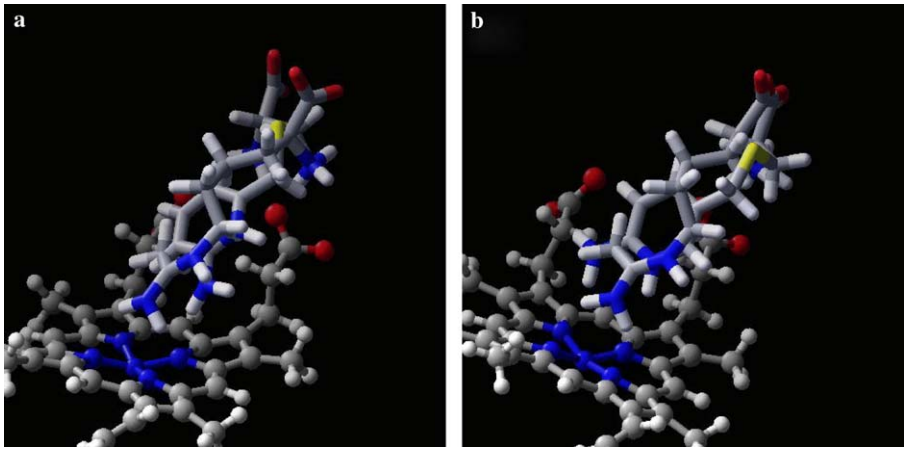


**Figure 4.** Superposition of the minimum energy conformations of **3**, **8**, and **10** in the iNOS active site. iNOS protein is not shown for the sake of clarity. Heme is displayed in ball and stick style. View of the conformations of (a) **3** and **8**; (b) **3** and **10** docked into the iNOS catalytic center.

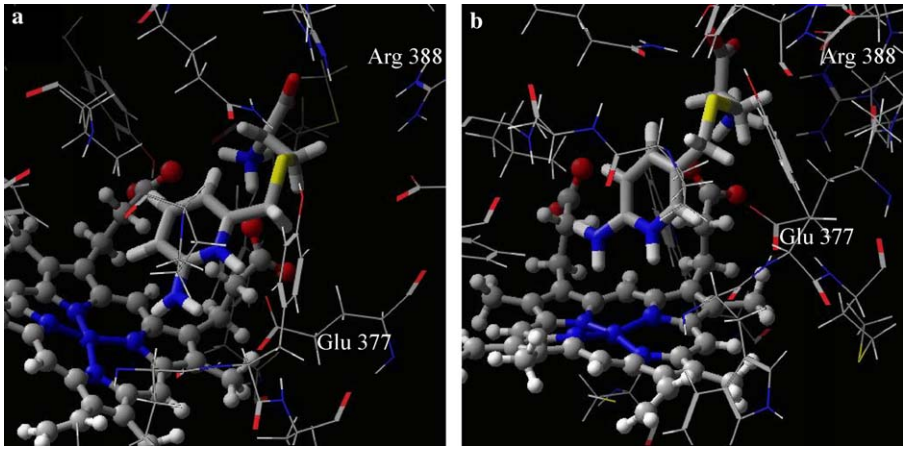


**Figure 5.** Superposition of the minimum energy conformations of **8** and **10**. View of the conformation of (a) **8** and (b) **10** docked into the iNOS catalytic center. Residues within 5 Å from the ligand are displayed using wire graphics and heme is displayed in ball and stick style.

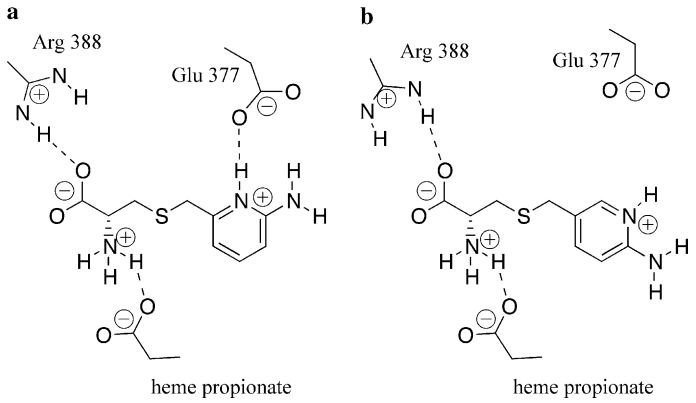


**Figure 6.** Hydrogen-bonding interactions of (a) **8** and (b) **10** with the iNOS active site.

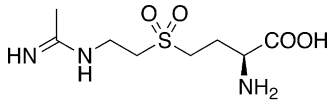

**21**: GW 274150

**Figure 7.** Structure of GW274150.

carboxylate was located at 5.11 Å from a hydrogen atom of Arg 388, and a hydrogen atom of ammonium ions were located at 1.42 and 1.48 Å from oxygen atoms of Glu 377. This result suggested that the tight binding to Glu 377 is important for the inhibition of NOS isozymes and the side-chain length of **8** is slightly short to bind two hydrogen atoms of pyridinium ion. However, two Arg residues (Arg 266 and Arg 388) are located near the carboxylate, and they might interact with carboxylate anion by ionic interaction. We further calculated the length between nitrogen atom of pyridine or iminoethyl moiety and carbon atom of carboxylate. The distance between nitrogen atom and carbon atom is 7.06 Å (**8**) and 8.13 Å (**21**), respectively. The distance between guanidium moiety and nitrogen atom of $\alpha$-$NH_3^+$ is 5.66 Å (**8**) and 7.38 Å (**21**), respectively. These results suggest that the longer side chain might be partially responsible for the better selectivity.

## 3. Conclusion

In summary, we have designed and synthesized various *S*-picolylcysteine-based compounds and examined their structure–activity relationship as human NOS inhibitors. Compound **8** had potent inhibitory activity toward all the human NOS isozymes, while **10** had low inhibitory activity. The results suggest that the amidino moiety of **8** is tightly bound to Glu 377 (iNOS) and the amino acid moiety interacts with Arg 388 (iNOS) and heme propionate, whereas the structure of **10** is less favorable for such interactions. Docking calculations were consistent with this view. In addition, the 2-methylpyridine derivative **11** had low activity, probably because of unfavorable interaction of the methyl group on the pyridine moiety with the human NOS binding site. This result suggests that an aminopyridine moiety at an appropriate position is favorable for recognition by human NOS. Compound **8** is a stable compound with potent inhibitory activity toward all of the human NOS isozymes and could be a useful scaffold for developing novel human NOS inhibitors. Further investigation of the structure–activity relationship is in progress in our laboratory and may lead to subtype-selective iNOS inhibitors.

## 4. Experimental

### 4.1. Chemistry

**4.1.1. General.** All manipulations were carried out under an argon atmosphere unless otherwise noted. Argon gas was dried by passage through $P_2O_5$ (Merck, SICAPENT). NMR spectra were recorded on a JEOL GSX-400 spectrometer (500 MHz for $^1$H, 100 MHz for $^{13}$C), JEOL JMN-LA500 spectrometer (400 MHz for $^1$H, 125 MHz for $^{13}$C), and JEOL JMN-AL500 spectrometer (500 MHz for $^1$H, 125 MHz for $^{13}$C). Chemical shifts are reported in $\delta$ parts per million referenced to an internal tetramethylsilane standard for $^1$H NMR. Chloroform-$d_1$ ($\delta$ 77.0 for $^{13}$C) was used as an internal reference for $^{13}$C NMR. $^1$H and $^{13}$C NMR spectra were recorded in $CDCl_3$ at 25 °C unless otherwise noted. IR spectra were obtained with a Jasco FT/IR-680 spectrometer, and values are expressed in $cm^{-1}$. Mass spectra were recorded on a JEOL JMS-LCmate and Bruker Daltonics APEX II mass spectrometer.

**4.1.2. Materials.** DMF (*N*,*N*-dimethylformamide) and dichloromethane were dried over calcium hydride and distilled prior to use. THF (tetrahydrofuran) and diethyl ether were dried over sodium benzophenone ketyl and distilled prior to use. Triethylamine and diisopropylethylamine were dried over KOH and distilled prior to use. Isobutene, di-*tert*-butyl dicarbonate ($Boc_2O$), picoline, 2-amino-4-picoline, 2-amino-6-picoline, 6-amino-3-picoline, and 2-6-lutidine were purchased from Tokyo Kasei Kogyo Co., Ltd. L-Cystine was purchased from Nacalai Tesque, Inc.

**4.1.3. General method for preparation of *N*,*N*-bis-*tert*-butyloxycarbonylamino-methylpyridines (14a–c).** A typical procedure, for the preparation of *N*,*N*-bis-*tert*-butyloxycarbonyl-2-amino-6-methylpyridine (**14a**) as an

example, is as follows. To a solution of 540 mg (5 mmol) of 2-amino-6-picoline and 12.2 mg (0.1 mmol) of DMAP in 10 mL of $CH_2Cl_2$ was added 1.05 mL of *N*,*N*-diisopropylethylamine at room temperature and the mixture was cooled to 0 °C. $Boc_2O$ 2.62 g (12 mmol) in 5 mL of $CH_2Cl_2$ was added and the reaction mixture was stirred for 6 h at room temperature. The reaction mixture was separated with 5% citric acid three times and then washed with sat. $NaHCO_3$ and brine. The organic phase was dried over $Na_2SO_4$ and the solvent was removed under reduced pressure. The residue was chromatographed on silica gel (eluent: hexane/EtOAc = 6:1) to give **14a** as a white solid, 338 mg (22%). The mono-Boc-protected compound was also obtained as a by-product, 415 mg (40%).

**4.1.3.1. *N*,*N*-Bis-*tert*-butyloxycarbonyl-2-amino-6-methylpyridine (14a).** Yield 22% as a white solid. $^1$H NMR ($CDCl_3$) $\delta$ 1.44 (s, 18H), 7.03 (d, $J$ = 7.8 Hz, 1H), 7.60 (d, $J$ = 7.8 Hz, 1H), 7.62 (t, $J$ = 7.8 Hz, 1H); MS (FAB) 331 (M+Na), 309 (M+H).

**4.1.3.2. *N*,*N*-Bis-*tert*-butyloxycarbonyl-2-amino-4-methylpyridine (14b).** Yield 33% as a colorless oil. $^1$H NMR ($CDCl_3$) $\delta$ 1.45 (s, 18H), 7.04 (m, 2H), 8.34 (d, $J$ = 5.4 Hz, 1H); MS (FAB) 331 (M+Na), 309 (M+H).

**4.1.3.3. *N*,*N*-Bis-*tert*-butyloxycarbonyl-6-amino-3-methylpyridine (14c).** Yield 24% as a white solid. $^1$H NMR ($CDCl_3$) $\delta$ 1.44 (s, 18H), 2.35 (s, 3H), 7.09 (d, $J$ = 8.2 Hz, 1H), 7.53 (dd, $J$ = 2.1 Hz, 8.2 Hz, 1H), 8.31 (d, $J$ = 2.1 Hz, 1H); MS (FAB) 331 (M+Na), 309 (M+H).

**4.1.4. General method for preparation of bromomethylpyridines (15a–c and 17d,e).** A typical procedure, for the preparation of 2-bromomethylpyridine (**17d**) as an example, is as follows. A solution of 0.5 mL (5 mmol) of picoline, 1.43 g (8 mmol) of *N*-bromosuccinimide, and 19.4 mg (0.08 mmol) of benzoyl peroxide in 40 mL $CCl_4$ was stirred at room temperature and then irradiated with a halogen lamp under reflux for 6 h. The reaction mixture was cooled and the precipitate was filtered off. The filtrate was concentrated under reduced pressure, and the residue was chromatographed on silica gel (eluent: $CH_2Cl_2$) to give 240 mg (28%) of **17d**.

**4.1.4.1. 2-Bromomethylpyridine (17d).** Yield 28% as a brown oil. $^1$H NMR ($CDCl_3$) $\delta$ 4.57 (s, 2H), 7.23 (m, 1H), 7.45 (m, 1H), 7.72 (m, 1H), 8.61 (m, 1H); FAB-MS was not detectable.

**4.1.4.2. 2-Bromomethyl-6-methylpyridine (17e).** Yield 36% as a brown powder. $^1$H NMR ($CDCl_3$) $\delta$ 2.56 (s, 3H), 4.52 (s, 2H), 7.07 (d, $J$ = 7.6 Hz, 1H), 7.24 (d, $J$ = 7.6 Hz, 1H), 7.58 (t, $J$ = 7.6 Hz, 1H); FAB-MS was not detectable.

**4.1.5. Preparation of (*R*)-*N*-*tert*-butoxycarbonyl-2-amino-3-[(2′-substituted-pyridyl)methylsulfanyl]propionic acid *O*-*tert*-butyl esters (19a–e).** A typical procedure, for the preparation of **19a** as an example, is as follows. To a solution of 193 mg (0.5 mmol) of **15a** and 348 μL (2.0 mmol) of *N*,*N*-diisopropylethylamine in 0.5 mL of $CH_2Cl_2$ was added 139 mg (0.5 mmol) of **18** at 0 °C, and the mixture was stirred for 18 h at room temperature. The solvent was removed under reduced pressure. The residue was chromatographed on silica gel (eluent: $CH_2Cl_2$/ethyl acetate = 9:1) to give **19a** as a colorless oil, 101 mg (35% in two steps).

**4.1.5.1. (*R*)-*N*-*tert*-Butoxycarbonyl-2-amino-3-{[2′-(*N*,*N*-bis-*tert*-butoxycarbonyl)aminopyrid-6′-yl]methylsulfanyl}propionic acid *O*-*tert*-butyl ester (19a).** Yield 35% as a colorless oil. $^1$H NMR ($CDCl_3$) $\delta$ 1.45 (s, 36H), 2.90 (m, 2H), 3.83 (s, 2H), 4.41 (m, 1H), 5.41 (br, 1H), 7.13 (d, $J$ = 7.8 Hz, 1H), 7.25 (d, $J$ = 7.8 Hz, 1H), 7.70 (t, $J$ = 7.8 Hz, 1H); MS (FAB) 606 (M+Na), 584 (M+H).

**4.1.5.2. (*R*)-*N*-*tert*-Butoxycarbonyl-2-amino-3-{[2′-(*N*,*N*-bis-*tert*-butoxycarbonyl)aminopyrid-4′-yl]methylsulfanyl}propionic acid *O*-*tert*-butyl ester (19b).** Yield 58% as a colorless oil. $^1$H NMR ($CDCl_3$) $\delta$ 1.45 (s, 18H), 1.46 (s, 9H), 1.47 (s, 9H), 2.79 (dd, $J$ = 5.6 Hz, 31.2 Hz, 2H), 3.73 (s, 3H), 4.41 (m, 1H), 5.33 (br, 1H), 7.20 (d, $J$ = 5.1 Hz, 1H), 7.22 (s, 1H), 8.41 (d, $J$ = 5.1 Hz, 1H); MS (FAB) 606 (M+Na), 584 (M+H).

**4.1.5.3. (*R*)-*N*-*tert*-Butoxycarbonyl-2-amino-3-{[2′-(*N*,*N*-bis-*tert*-butoxycarbonyl)aminopyrid-5′-yl]methylsulfanyl}propionic acid *O*-*tert*-butyl ester (19c).** Yield 53% as a colorless oil. $^1$H NMR ($CDCl_3$) $\delta$ 1.44 (s, 18H), 1.46 (s, 9H), 1.47 (s, 9H), 2.81 (dd, $J$ = 5.6 Hz, 31.2 Hz, 2H), 3.77 (s, 3H), 4.43 (m, 1H), 5.30 (br, 1H), 7.20 (d, $J$ = 8.3 Hz, 1H), 7.71 (d, $J$ = 8.3 Hz, 1H), 8.40 (s, 1H); MS (FAB) 584 (M+H).

**4.1.5.4. (*R*)-*N*-*tert*-Butoxycarbonyl-2-amino-3-{(pyrid-2′-yl)methylsulfanyl}propionic acid *O*-*tert*-butyl ester (19d).** Yield 35% as a colorless oil. $^1$H NMR ($CDCl_3$) $\delta$ 1.45 (s, 18H), 2.93 (d, $J$ = 5.4 Hz, 2H), 3.88 (s, 2H), 4.42 (m, 1H), 5.68 (br, 1H), 7.17 (m, 1H), 7.32 (m, 1H), 7.66 (m, 1H), 8.55 (m, 1H); MS (FAB) 369 (M+H).

**4.1.5.5. (*R*)-*N*-*tert*-Butoxycarbonyl-2-amino-3-{(2′methyl-pyrid-6′-yl)methylsulfanyl}propionic acid *O*-*tert*-butyl ester (19e).** Yield 36% as a colorless oil. $^1$H NMR ($CDCl_3$) $\delta$ 1.45 (s, 18H), 2.56 (s, 3H), 2.91 (m, 2H), 3.84 (s, 2H), 4.43 (m, 1H), 5.98 (br, 1H), 7.03 (d, $J$ = 7.8 Hz, 1H), 7.12 (d, $J$ = 7.8 Hz, 1H), 7.54 (t, $J$ = 7.8 Hz, 1H); MS (FAB) 383 (M+H).

**4.1.6. Preparation of (*R*)-*N*-*tert*-butoxycarbonyl-2-amino-3-(pyrid-2′-ylmethylsulfonyl)propionic acid *O*-*tert*-butyl ester (20).** To a solution of 66 mg (0.18 mmol) of **19a** in 5 mL of $CH_2Cl_2$ was added 78 mg (0.45 mmol) of *m*-CPBA and the mixture was stirred at room temperature for 3 h. It was then diluted with $CH_2Cl_2$ and washed with saturated $NaHCO_3$ three times and brine once. The organic layer was dried over $Na_2SO_4$ and concentrated under reduced pressure. The residue was chromatographed on silica gel (eluent: $CH_2Cl_2$/EtOAc = 1:1) to give **20** as a colorless oil, 23.4 mg (32%).

$^1$H NMR ($CDCl_3$) $\delta$ 1.45 (s, 9H), 1.46 (s, 9H), 3.64 (m, 2H), 4.50 (m, 2H), 4.66 (m, 1H), 5.99 (br, 1H), 7.33 (m,

1H), 7.46 (d, $J = 7.6$ Hz, 1H), 7.77 (m, 1H), 8.64 (m, 1H); MS (FAB) 423 (M+Na), 401 (M+H).

**4.1.7. Preparation of (*R*)-2-amino-3-[(2′-substituted-pyridyl)methylsulfanyl]propionic acid dihydrochlorides (7–12).** A typical procedure, for the preparation of **7** as an example, is as follows. HCl-saturated 1,4-dioxane solution (5 mL) was added to 51 mg (0.14 mmol) of **18d** at 0 °C and the mixture was stirred for 12 h at room temperature. The solvent was removed under reduced pressure and 40 mg (quantitative) of the desired compound **7** was obtained. Upon recrystallization from MeOH–ether, 12 mg of **7** was obtained as a light yellow solid. Purity was confirmed by HPLC.

**4.1.7.1. (*R*)-2-Amino-3-[(pyrid-2′-yl)methylsulfanyl]-propionic acid dihydrochloride (7).** Yield quant. as a brown powder. $^1$H NMR ($CD_3OD$) $\delta$ 3.08 (dd, $J = 7.6$ Hz, 14.9 Hz, 1H), 3.21 (dd, $J = 4.4$ Hz, 14.9 Hz, 1H), 4.27 (s, 2H), 4.35 (t, $J = 4.4$ Hz, 1H), 7.97 (m, $J = 7.3$ Hz, 7.8 Hz, 1H), 8.08 (d, $J = 7.8$ Hz, 1H), 8.56 (d, $J = 7.8$ Hz, 1H), 8.82 (d, $J = 7.3$ Hz, 1H); $^{13}$C NMR ($CD_3OD$) $\delta$ 32.7, 33.7, 53.2, 127.2, 128.9, 143.6, 148.3, 154.7, 170.0; IR (KBr) 1734, 2360, 3425 cm$^{-1}$; MS (FAB) 235 (M+Na), 213 (M+H); Anal. Calcd for $C_9H_{12}N_2O_2S{\cdot}2HCl$: C, 37.90; H, 4.95; N, 9.82. Found: C, 37.33; H, 5.03; N, 9.63.

**4.1.7.2. (*R*)-2-Amino-3-[(2′-aminopyrid-6′-yl)methylsulfanyl]propionic acid dihydrochloride (8).** Yield quant. as a light brown powder. $^1$H NMR ($CD_3OD$) $\delta$ 3.03 (m, 1H), 3.14 (m, 1H), 3.94 (s, 2H), 4.31 (m, 1H), 6.86 (d, $J = 7.3$ Hz, 1H), 6.93 (d, $J = 8.3$ Hz, 1H), 7.86 (dd, $J = 7.3$ Hz, 8.3 Hz, 1H); $^{13}$C NMR ($CD_3OD$) $\delta$ 32.2, 33.2, 54.2, 113.6, 113.7, 117.6, 145.4, 146.7; IR (KBr) 1662, 2361, 3397 cm$^{-1}$; MS (FAB) 228 (M+H); Anal. Calcd for $C_9H_{13}N_3O_2S{\cdot}2HCl{\cdot}0.6H_2O$: C, 34.76; H, 5.25; N, 13.51. Found: C, 34.99; H, 5.91; N, 12.91.

**4.1.7.3. (*R*)-2-Amino-3-[(2′-aminopyrid-4′-yl)methylsulfanyl]propionic acid dihydrochloride (9).** Yield quant. as an off-white powder. $^1$H NMR ($CD_3OD$) $\delta$ 3.00 (dd, $J = 7.6$ Hz, 14.9 Hz, 1H), 3.11 (dd, $J = 4.3$ Hz, 14.9 Hz, 1H), 3.86 (s, 2H), 4.26 (dd, $J = 4.3$ Hz, 7.6 Hz, 1H), 6.94 (d, $J = 6.7$ Hz, 1H), 7.23 (s, 1H), 7.80 (d, $J = 6.7$ Hz, 1H); $^{13}$C NMR ($CD_3OD$) $\delta$ 32.4, 35.8, 53.2, 113.9, 114.7, 136.6, 155.7, 157.7, 170.2; IR (KBr) 1669, 2360, 3427 cm$^{-1}$; MS (FAB) 228 (M+H); Anal. Calcd for $C_9H_{13}N_3O_2S{\cdot}2HCl{\cdot}0.75H_2O$: C, 34.46; H, 5.30; N, 13.39. Found: C, 34.48; H, 5.67; N, 12.91.

**4.1.7.4. (*R*)-2-Amino-3-[(2′-aminopyrid-5′-yl)methylsulfanyl]propionic acid dihydrochloride (10).** Yield quant. as a brown powder. $^1$H NMR ($CD_3OD$) $\delta$ 2.98 (dd, $J = 7.6$ Hz, 14.9 Hz, 1H), 3.09 (dd, $J = 4.2$ Hz, 14.9 Hz, 1H), 3.79 (s, 2H), 4.27 (dd, $J = 4.2$ Hz, 7.6 Hz, 1H), 7.04 (d, $J = 9.4$ Hz, 1H), 7.83 (s, 1H), 8.00 (d, $J = 9.4$ Hz, 1H); $^{13}$C NMR ($CD_3OD$) $\delta$ 32.4, 33.4, 53.2, 115.5, 124.1, 135.0, 144.9, 146.7, 155.2; IR (KBr) 1671, 2360, 3853 cm$^{-1}$; MS (FAB) 228 (M+H); Anal. Calcd for $C_9H_{13}N_3O_2S{\cdot}2HCl{\cdot}H_2O$: C, 33.97; H, 5.39; N, 13.21. Found: C, 34.38; H, 5.57; N, 12.85.

**4.1.7.5. (*R*)-2-Amino-3-[(2′-methyl-pyrid-6′-yl)methylsulfanyl]propionic acid dihydrochloride (11).** Yield quant. as a brown powder. $^1$H NMR ($CD_3OD$) $\delta$ 2.83 (s, 3H), 3.17 (m, 2H), 4.26 (m, 2H), 4.37 (m, 1H), 7.84 (m, 1H), 7.94 (m, 1H), 8.44 (m, 1H); $^{13}$C NMR ($CD_3OD$) $\delta$ 26.4, 32.6, 33.3, 53.2, 126.0, 127.9, 147.9, 156.4; IR (KBr) 1636, 2361, 3420 cm$^{-1}$; MS (FAB) 227 (M+H); HR-MS (ESI) Calcd for $C_{10}H_{15}N_2O_2S$: 227.0849 (M+H). Found: 227.0876.

**4.1.7.6. (*R*) 2-Amino-3-(pyrid-2′-ylmethylsulfonyl)propionic acid dihydrochloride (12).** Yield quant. as a brown powder. $^1$H NMR ($CD_3OD$) $\delta$ 3.84 (m, 1H), 4.18 (m, 1H), 4.74 (m, 1H), 7.94 (m, 1H), 8.03 (d, $J = 7.8$ Hz, 1H), 8.45 (m, 1H), 8.87 (m, 1H); $^{13}$C NMR ($CD_3OD$) $\delta$ 53.4, 127.6, 130.4, 145.4, 146.7, 168.8; IR (KBr) 1636, 2360, 3445 cm$^{-1}$; MS (FAB) 245 (M+H); HR-MS (ESI) Calcd for $C_9H_{13}N_2O_4S$: 245.05941 (M+H). Found: 245.0625.

### 4.2. Measurement of NOS-inhibitory activity

**4.2.1. Materials.** Ex-cell 420 was purchased from JRH Biosciences. Hemin was purchased from Tokyo Kasei Kogyo Co., Ltd. Riboflavin, nicotinic acid, $BH_4$, DTT, and PMSF were purchased from Wako Pure Chemical Industries, Ltd, and Tris–HCl, EGTA, FAD, and FMN from Nacalai Tesque, Inc. CHAPS was purchased from Dojindo Laboratories. Pepstatin, leupeptin, and chymostatin were purchased from Peptide Institute, Inc. 2′,5′-ADP Sepharose was purchased from Pharmacia Biotech and NADPH from Oriental Yeast Co., Ltd.

**4.2.2. Expression and purification of human NOS isozymes.** Human NOS isozymes were expressed in Sf-9 (a *Spodoptera frugiperda* insect cell line) as previously reported.[15] Monolayer cultures of Sf-9 cells were infected with human NOS recombinant baculovirus and incubated for 72 h at 27 °C in Ex-cell 420 insect serum-free medium supplemented with 1.5 μg/mL hemin, 1 μM riboflavin, 5 μM nicotinic acid, and 10 μM $BH_4$. For iNOS, Sf-9 cells were co-infected with the CaM baculovirus. The cells were harvested by centrifugation and homogenized in five volumes of ice-cold buffer (Tris–HCl 50 mM, pH 7.5, containing 1 mM EGTA, 1 mM DTT, 1 mM PMSF, 1 μg/mL pepstatin, 1 μg/mL leupeptin, 20 μM chymostatin, 5 μM FAD, 5 μM FMN, and 10 μM $BH_4$; for eNOS, 10 mM CHAPS was included). The homogenate was centrifuged at 40,000*g* for 30 min. The supernatant fractions were applied to a 2 mL 2′,5′-ADP Sepharose affinity column. The column was washed with 0.5 M NaCl and eluted with 10 mM NADPH. The eluted fraction was concentrated to 0.2 mg/mL with a Centricon 30. For eNOS, 10 mM CHAPS was included in the buffer to obtain sufficient solubility of the enzyme.

**4.2.3. Enzyme assay and $K_i$ values.** Recombinant human NOS activity was measured by monitoring the conversion of [$^{14}$C]-L-citrulline as previously reported.[15] Enzyme solution (5 μL) was added to 25 μL of buffer containing 50 mM HEPES (pH 7.4), 4.2–16.7 μM [$^{14}$C]-L-arginine, 18 mM $CaCl_2$, 150 μM DTT, 10 μg/mL CaM, 15 μM $BH_4$, 1 mM EGTA, 15 μM FAD, 15 μM FMN, 0.9 mg/

mL BSA, 1.5 mM NADPH, and the test compound in the concentration range from 1 pM to 1 mM. After incubation for 10 min at 37 °C, the reaction was terminated by adding 20 μL of 5 mM cold L-arginine and 5 mM L-citrulline, and boiling the mixture at 95 °C for 5 min. An aliquot (3 μL) was spotted onto a cellulose plate and separated by thin-layer chromatography using methanol–pyridine–water (25:2:5, v/v/v). Radioactivity was measured by autoradiography with a Fuji BAS 2500 Bioimaging analyzer. The $IC_{50}$ values of the inhibitors were calculated by means of linear regression using the data points just above and below 50% activity. The kinetic data were obtained by Dixon analysis. Calculations were performed using Excel and Igor software.

### 4.3. Molecular modeling

Docking was performed using MacroModel 8.1 software. Coordinates of rat nNOS, human iNOS, and human eNOS complexed with arginine or hydroxyarginine were taken from the Protein Data Bank (PDB code 1NSI) and hydrogen atoms were added computationally at appropriate positions. The structures of L-NIL (**3**) and compounds **8**, **10**, and **21** docked to NOS were constructed by molecular mechanics (MM) energy minimization. The starting positions of **3**, **8**, **10**, and **21** were determined manually. The conformations of **3**, **8**, **10**, and **21** in the active site were minimized by MM calculation based upon the OPLS-AA force field.

## Acknowledgments

We thank Dr. Takayoshi Suzuki and Professor Naoki Miyata of this university for the docking study, and Mr. Takehiro Yamane for assistance in synthesizing protected picolines. We are grateful to Uehara Memorial Foundation for financial support.

## References and notes

1. Moncada, S.; Palmer, R. M.; Higgs, E. A. *Pharmacol. Rev.* **1991**, *43*, 109–142.
2. Marletta, M. A. *J. Med. Chem.* **1994**, *37*, 1899–1907.
3. Moncada, S.; Higgs, E. A. *FASEB J.* **1995**, *9*, 1319–1930.
4. Nathan, C. *J. Clin. Invest.* **1997**, *100*, 2417–2423.
5. Forstermann, U.; Pollock, J. S.; Schmidt, H. H.; Heller, M.; Murad, F. *Proc. Natl. Acad. Sci. U.S.A.* **1991**, *88*, 1788–1792.
6. Babu, B. R.; Griffith, O. W. *Curr. Opin. Chem. Biol.* **1998**, *2*, 491–500.
7. MacMicking, J.; Xie, Q. W.; Nathan, C. *Annu. Rev. Immunol.* **1997**, *15*, 323–350.
8. Nathan, C.; Xie, Q. W. *Cell* **1994**, *78*, 915–918.
9. Alderton, W. K.; Cooper, C. E.; Knowles, R. G. *Biochem. J.* **2001**, *357*, 593–615.
10. Narayanan, K.; Spack, L.; McMillan, K.; Kilbourn, R. G.; Hayward, M. A.; Masters, B. S. S.; Griffith, O. W. *J. Biol. Chem.* **1995**, *270*, 11103–11110.
11. Moore, W. M.; Webber, R. K.; Jerome, G. M.; Tjoeng, F. S.; Misko, T. P.; Currie, M. G. *J. Med. Chem.* **1994**, *37*, 3886–3888.
12. Stuehr, D. J.; Griffith, O. W. *Adv. Enzymol.* **1992**, *65*, 287–346.
13. Garvey, E. P.; Oplinger, J. A.; Furfine, E. S.; Kiff, R. J.; Laszlo, F.; Whittle, B. J.; Knowles, R. G. *J. Biol. Chem.* **1997**, *272*, 4959–4963.
14. Kobayashi, N.; Higuchi, T.; Urano, Y.; Kikuchi, K.; Hirobe, M.; Nagano, T. *Biol. Pharm. Bull.* **1999**, *22*, 936–940.
15. Park, J.-M.; Higuchi, T.; Kikuchi, K.; Urano, Y.; Hori, H.; Nishino, T.; Aoki, J.; Inoue, K.; Nagano, T. *Br. J. Pharmacol.* **2001**, *132*, 1876–1882.
16. Ijuin, R.; Umezawa, N.; Nagai, S.; Higuchi, T. *Bioorg. Med. Chem. Lett.* **2005**, *15*, 2881–2885.
17. Connolly, S.; Aberg, A.; Arvai, A.; Beaton, H. G.; Cheshire, D. R.; Cook, A. R.; Cooper, S.; Cox, D.; Hamley, P.; Mallinder, P.; Millichip, I.; Nicholls, D. J.; Rosenfeld, R. J.; St-Gallay, S. A.; Tainer, J.; Tinker, A. C.; Wallace, A. V. *J. Med. Chem.* **2004**, *47*, 3320–3323.
18. Bisacchi, G. S.; Slusarchyk, W. A.; Bolton, S. A.; Hartl, K. S.; Jacobs, G.; Mathur, A.; Meng, W.; Ogletree, M. L.; Pi, Z.; Sutton, J. C.; Treuner, U.; Zahler, R.; Zhao, G.; Seiler, S. M. *Bioorg. Med. Chem. Lett.* **2004**, *14*, 2227–2231.
19. Olsen, R. K.; Kini, G. D.; Hennen, W. J. *J. Org. Chem.* **1985**, *50*, 4332–4336.
20. Wilson, J. G.; Cohen, L. A. *J. Am. Chem. Soc.* **1963**, *85*, 560–564.
21. Hori, H.; Iwasaki, T.; Kurahashi, Y.; Nishino, T. *Biochem. Biophys. Res. Commun.* **1997**, *234*, 476–480.
22. Dixon, M. *Biochem. J.* **1953**, *55*, 170–171.
23. Li, H.; Raman, C. S.; Glaser, C. B.; Blasko, E.; Young, T. A.; Parkinson, J. F.; Whitlow, M.; Poulos, T. L. *J. Biol. Chem.* **1999**, *274*, 21276–21284.
24. Alderton, W. K.; Angell, A. D. W.; Craig, C.; Dawson, J.; Garvey, E.; Moncada, S.; Monkhouse, J.; Rees, D.; Russell, L. J.; Russell, R. J.; Schwartz, S.; Waslidge, N.; Knowles, R. G. *Br. J. Pharmacol.* **2005**, *145*, 301–312.